Dynamical scaling and the growth of diffusion-limited aggregates

H. G. E. Hentschel and J. M. Deutch
Department of Chemistry, Massachusetts Institute of Technology, Cambridge, Massachusetts 02139

Paul Meakin
Central Research and Development Department,[a] Experimental Station, E. I. du Pont de Nemours and Company, Inc., Wilmington, Delaware 19898

(Received 16 March 1984; accepted 22 May 1984)

The validity of dynamical scaling for the growth of aggregates in a bath of particles of concentration c_0 is investigated. A length scale $\xi \sim c_0^{-1/(d-D)}$ is introduced which governs the crossover from a fractal of dimension D to compact aggregate behavior. For static scaling a variable $x = R/\xi$ is introduced where R is the radius of gyration of the aggregate. The cluster size N is found to vary as $N(c_0,R) = (\xi/a)^D x^D g(x)$, where a is the particle size and the static structure function is well represented by $g(x) = (A + Bx)^{d-D}$. To consider dynamical scaling the asymptotic dynamics are first examined. For $R \ll \xi$ the radius of gyration and cluster size are respectively found to grow with time as $R(c_0,t) \sim (c_0 t)^{1/(2+D-d)}$ and $N(c_0,t) \sim (c_0 t)^{D/(2+D-d)}$. While for $R \gg \xi$ one finds $R(c_0,t) \sim c_0^{1/(d-D)} t$ and $N(c_0,t) \sim c_0^{1+d/(d-D)} t^d$. If a scaled time variable $\tau = D_f t/\xi^2$ is introduced where D_f is a microscopic diffusion constant, then the previous asymptotic results can be incorporated into dynamical scaling forms for $R(c_0,t)$ and $N(c_0,t)$. These are $R(c_0,t)/\xi = x = \tau^{1/(2+D-d)} f_1(\tau)$ where $f_1(\tau)$ is well represented by the form $f_1(\tau) = [A_1 + B_1\tau]^{1-1/(D+2-d)}$; while $N(c_0,t) = (\xi/a)^D \tau^{D/(2+D-d)} f_2(\tau)$ where $f_2(\tau)$ can be written $[A_2 + B_2\tau]^{d-D/(2+D-d)}$. Using these results all concentration c_0 and time t regimes can be investigated. Dynamical scaling is found to hold within the errors inherent in computer simulations due to depletion effects of finite lattices.

I. INTRODUCTION

Recently Witten and Sander[1] introduced a model for the growth of aggregates. A seed particle is placed at a lattice site and a random walk is released isotropically from a long distance off. If it reaches a nearest-neighbor site, it becomes part of the growing cluster; if not, it is killed off and a new particle released. Computer simulations[2] have shown that the aggregates so formed have a complex random dendritic structure with interesting scaling properties—they are fractals.[3] The fractal objects can be categorized by the relationship $N \sim (R/a)^{D(d)}$, where N is the number of particles in the growing cluster, R is its radius of gyration, a is the length scale of the diffusing single particles, and $D(d)$ is the fractal dimension of the cluster grown in a d dimensional space. Computer simulations[2] suggest $D \approx 5d/6$ while different assumptions about the structure of this aggregate lead theoretically,[4–6] to $D(d) = (d^2+1)/(d+1)$ or $D(d) = (8+5d^2)/(6+5d)$.

However, while the Witten–Sander model provides valuable insights into the structure of diffusion-limited aggregates; as a model for growth and morphology one would expect to have to modify the model in one of two crucial ways.

First, if one wants a model for colloidal flocculation or coagulation, the aggregates do not grow on a single seed particle, but rather from an initial concentration c_0 of particles in a medium. In the medium, all particles, or clusters can collide and become irreversibly joined. Thus aggregates do not in general grow by the diffusion of particles to a single growing cluster but rather by cluster–cluster aggregation. In fact, computer simulations[7–9] suggest that the aggregates so formed are much more "stringy" than those found in the case of single cluster aggregation and their fractal dimensions are considerably lower. Theoretically[10] one would expect these aggregates to belong to a different universality class from those formed by single particle aggregation with $D(d) = d(4d+3)/(9d-2)$ for $d < 8$, and $D(d) = d/2$ for $d > 8$.

Second, in those cases where aggregates can only grow from some unique site one would still not expect particles to be introduced one at a time. Rather the simplest physical assumption would be that there exists a bath of particles of concentration c_0 which can diffuse into the growing aggregate, and whose volume is so large that one can neglect depletion effects. This model introduced by Meakin and Witten[11] is fundamentally different from the Witten–Sander model in so far as it has a dynamics associated with it. Namely, in this case, the aggregate grows at a rate determined by the absorbtion of the flux of particles created by the gradient in the particle bath concentration due to the existence of the absorbing aggregate. In the original Witten–Sander model, in contrast, it does not matter how long a diffusing particle takes to reach a nearest-neighbor site of the aggregate, or even if it does so. In fact, the Witten–Sander is actually an algorithm for the probability of a given configuration of joined particles.

The time dependence of the above mentioned generalization has been investigated numerically by Meakin and Deutch[12] with the result for the growth law[13] of the radius of gyration

$$R(t) \sim t^{[1/(2+D-d)]} \tag{1.1}$$

[a] Contribution No. 3451

 0021-9606/84/172496-07$02.10

for short enough times which depend on the concentration c_0 of the particle bath. At long times one finds from computer simulations[11] $R(t) \sim t$ for all dimensions d.

To account for this crossover behavior and find both the time t and concentration c_0 dependence for the growth rates of the radius of gyration $R(c_0,t)$ and the number of particles in the cluster $N(c_0,t)$ in all time and concentration regimes is the object of this paper. We accomplish this by noting that there exists a unique length side $\xi \sim a(c_0 a^d)^{-1/(d-D)}$ associated with this model. We derive this length scale in Sec. II and consider the validity of static scaling by a comparison with the earlier computer simulations.[12] A form for the static structure function is suggested, which agrees well with the computer data, by the use of Padé approximants.

In Sec. III we consider the asymptotic time dependence of the radius of gyration $R(c_0,t)$ and the cluster size $N(c_0,t)$ in the regimes $R \ll \xi$ and $R \gg \xi$. We note that these are consistent with dynamical scaling and this hypothesis is investigated by a comparison with computer simulations.[12] The forms of the relevant dynamic structures function can be found by fitting their logarithmic derivatives by Padé approximants as their asymptotic behavior is known. The agreement with computer simulations is satisfactory.

Finally, in Sec. IV we summarize our results and offer some concluding remarks.

II. STATIC SCALING

We consider an initiating seed in a bath of particles of concentration c_0. The growth of the aggregate occurs by the diffusion of particles from the bath which irreversibly stick to the aggregate on contact. Initially the concentration of particles in the aggregate satisfies the condition $N/R^d \gg c_0$ which is essentially the conditions of growth of the Witten–Sander model.[1] Thus, if a is the length scale of the diffusing particles, then we expect

$$N \sim (R/a)^D, \tag{2.1}$$

where $\sim$ means "scales-like" and D is the fractal dimension of the aggregate in the Witten–Sander model.

However, the behavior given by Eq. (2.1) cannot continue forever in any bath of finite concentration c_0. This is because apart from aggregate growth by the irreversibly sticking of single particles which will create a Witten–Sander cluster, a second mechanism for aggregate growth always exists at finite bath concentration c_0. When one particle becomes the nearest neighbor of the growing aggregate and sticks irreversibly, so do its nearest-neighbor bath particles which now in turn have suddenly also become nearest neighbors of the aggregate. In addition regions of density c_0 can be caged by the growing arms of the aggregate thus ensuring their whole scale incorporation into the aggregate. Thus whole regions of density c_0 become part of the growing aggregate and consequently $N/R^d \gtrsim c_0$. When $N/R^d \gg c_0$ this effect is insignificant and Witten–Sander growth $N \sim R^D$ results. However, as $D < d$ this relationship cannot continue forever and for large R in contrast with Eq. (2.1), we would expect the aggregation of density c_0 to dominate resulting in a compact structure obeying

$$N \sim c_0 R^d. \tag{2.2}$$

The crossover between these two limiting cases occurs at a unique length scale ξ which occurs when the concentration of the aggregate reduces to the external concentration $N_\xi/\xi^d \sim c_0$ or

$$(\xi/a)^D \xi^{-d} \sim c_0, \tag{2.3a}$$

$$\xi \sim a(c_0 a^d)^{-1/(d-D)}. \tag{2.3b}$$

The fact that crossover to constant density occurs in baths of finite concentrations has already been observed in the context of continuum models of DLA.[14,15] These models have not been shown to create Witten–Sander-like structures, but the spherically symmetric solutions of the nonlinear partial differential equations which represent the model do behave in certain respects like fractals with $D = d - 1$. A divergent boundary layer with width $\xi \sim c_0^{-\theta}$, where $\theta = 1$ exists in this model and gives the crossover to constant density. This result is consistent with Eq. (2.3b) where $\theta = 1/(d - D)$.

We introduce the static scaling hypothesis that ξ is the only relevant length scale for this model, in which case

$$N(c_0,R) = (R/a)^D g(R/\xi) = (\xi/a)^D G(R/\xi), \tag{2.4}$$

where $g(x)$ contains the deviation from the Witten–Sander model while $G(x) = x^D g(x)$ describes the behavior of the cluster size with the radius of gyration. The limiting forms for N are given, respectively, by Eq. (2.1) for $R \ll \xi$ and by Eq. (2.2) for $R \gg \xi$ so that $g(x)$ must have the asymptotic forms $g(x) \sim$ constant as $x \to 0$ and $g(x) \sim x^{d-D}$ as $x \to \infty$.

To test this hypothesis we show in Fig. 1(a) the original computer simulations[12] of the dependence of the radius of gyration R on cluster size N for two-dimensional lattice models of the diffusion-limited aggregation in the form of log–log plots, where curves A,B,C, and D represent, respectively, concentrations per lattice site $\rho = (c_0 a^d)$ of 0.0625, 0.125, 0.25, and 0.3125. Four distinct curves can be seen. In Fig. 1(b) we have replotted the data using the scaling variables $N/(R/a)^D$ vs $(R/a)\rho^{-1/(d-D)}$ again in the form of log–log plots. The exponent $1/(d-D)$ is very sensitive to the value chosen for D [when $d = 2$, $D = 1.67$ then $1/(d-D) = 3$; while if D 1.75 is chosen then $1/(d-D) = 4$]. Thus, if scaling is valid, then accurate simulation data could be used to distinguish between different theoretical possibilities for D. However, as real computer simulations suffer from depletion effects (when the majority of the reservoir particles are incorporated into the growing aggregate), this approach is not open to us and instead we shall use the best values from computer simulations[2] $D(2) = 1.67, D(3) = 2.50$ in our comparison of scaling predictions with computer data. When we use this value for $D(2)$ in Fig. 1(b), all the data lie on a single curve within experimental error, confirming the static scaling hypothesis. A specific form for $g(x)$ is also included in Fig. 1(b). This form is determined as follows: We know the asymptotic form for $g(x)$, namely, $g(x) \to$ constant as $x \to 0$ and $g(x) \sim x^{d-D}$ as $x \to \infty$. Therefore, we might try to approximate the function $g(x)$ by $A + Bx^{d-D}$ over the whole range of x. However, this cannot be correct as it suggests that $g(x)$ has singular behavior at $x = 0$, while there is no reason to believe that $g(x)$ is anything but analytic as $x \to 0$, the singularities occurring as $x \to \infty$. Neither can $g(x)$ be represent-

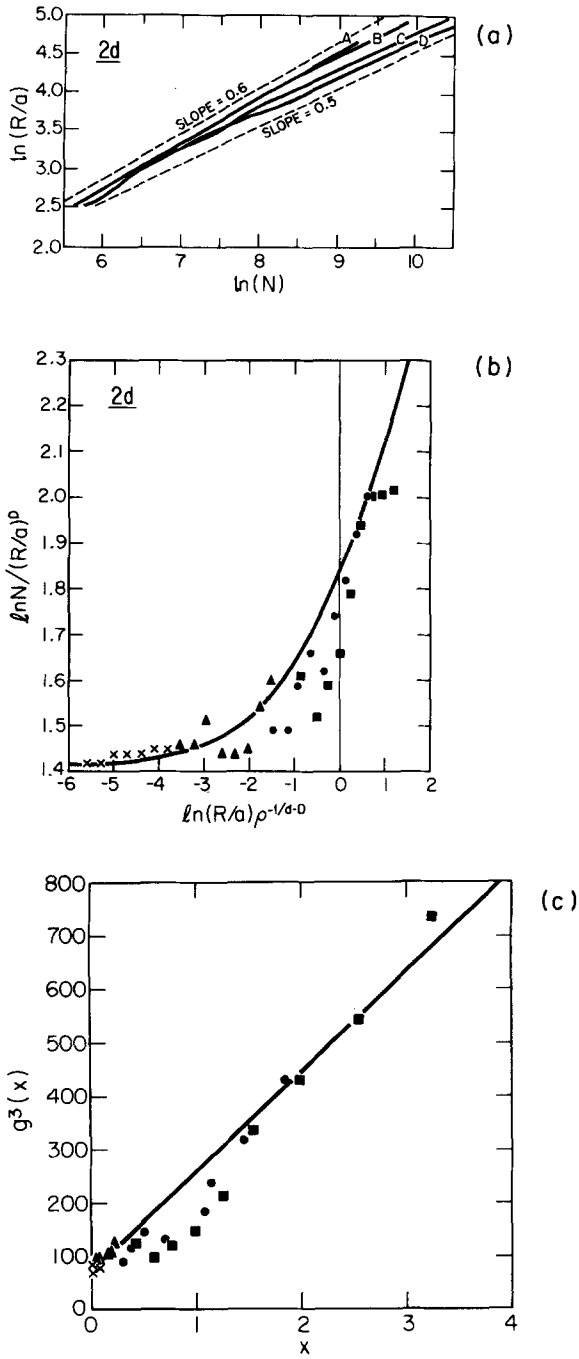

FIG. 1. (a) Dependence of radius of gyration (R/a) on cluster size N for two dimensional lattice models of diffusion limited aggregation in the form of log–log plots. The simulations were carried out on a 400×400 square lattice with one seed and a variable number of particles which were present at all times as either mobile particles or as part of the cluster grown from the seed. Curve A shows the results for 10 000 particles ($\rho = 0.0625$); curve B for $\rho = 0.125$ (20 000 particles); curve C for $\rho = 0.25$ (40 000 particles); and curve D for $\rho = 0.3125$ (50 000 particles). The straight lines with slopes 0.6 and 0.5 show the limiting behaviors of R with N. (b) Data from the four curves in Fig. 1(a) have been taken and replotted in Fig. 1(b) in a log–log form using the scaling variables $N/(R/a)^D$ vs $x = (R/a)\rho^{-1/(d-D)}$. Points from the curves A,B,C,D are represented respectively by the symbols $\times$,▲,●,■. The data should fall on a universal curve. The theoretical form of this curve is $\ln g(x)$ where $g(x) = [A + Bx]^{1/3}$. This curve is also drawn with $A = 70, B = 185$. (c) The same data which appears in Fig. 1(b) has been replotted in a different form. $[N/(R/a)^D]^{1/(d-D)}$ has been plotted against $x = (R/a)\rho^{-1/(d-D)}$ (with $d = 2$, $D = 5/3$). The ordinate should theoretically be $g(x)^{1/(d-D)} = [A + Bx]$ while the abscissa is x. Thus the data should line on a universal straight line. The line $[70 + 185x]$ has been drawn for comparison.

ed by a Padé approximant. However, such functions which exhibit nonanalytic singularities also appear in the theory of critical phenomena, but as is well known,[16] in general, their logarithmic derivatives can be analytically represented. Thus as $d\ln g/dx \to$ constant as $x \to 0$ and $d\ln g/dx \to (d - D)/x$ as $x \to \infty$, the simplest Padé approximant we could choose would be $d\ln g/dx = (d - D)/(a_0 + x)$ or

$$g(x) = [A + Bx]^{(d-D)}, \tag{2.5}$$
$$G(x) = x^D [A + Bx]^{(d-D)},$$

where A and B are constants which must be found experimentally.

To check the form (2.5) in the two dimensional case we have replotted the data in Fig. 1(b) in the form of $g^3(x)$ vs x in Fig. 1(c) [since $(d - D) = 1/3$ for $d = 2$]. The points should fall on the straight line $[A + Bx]$ and this appears to be the case within experimental accuracy with $A = 70$ and $B = 185$. These values are used in Fig. 1(b) for the theoretical curve. Clearly static scaling holds and this encourages us to investigate the validity of dynamical scaling for the growing clusters.

III. DYNAMIC SCALING

Before we introduce the dynamic scaling hypothesis, consider the asymptotic time and concentration dependence of the radius of gyration $R(c_0,t)$ and the cluster size $N(c_0,t)$ in the regimes $R \ll \xi$ and $R \gg \xi$.

A. The $R \ll \xi$ regime

The dynamics in this regime have been considered by Deutch and Meakin.[11] Here the concentration of the aggregate particles $N/R^d \gg c_0$ and particles from the medium do not penetrate the cluster. One expects the flux J_1 of particles entering through a conceptual spherical surface R surrounding the aggregate to be absorbed on the surface

$$dN/dt = J_1. \tag{3.1}$$

The steady-state spherically symmetric flux J_1 has been calculated[13] from the concentration gradient that is set up by this absorption. This concentration gradient can be obtained from the steady state solution of the d dimensional diffusion equation

$$\frac{1}{r^{d-1}}\frac{d}{dr}r^{d-1}\frac{dc}{dr} = 0 \tag{3.2}$$

subject to the boundary conditions $c(R) = 0$, $c(r) \to c_0$ as $r \to \infty$. The result is

$$J_1 \sim D_f c_0 R^{d-2}, \tag{3.3}$$

where D_f is the diffusion constant (for a jump model where particles hop at random by a distance a in time τ_0 we would have $D_f = a^2/\tau_0$). On substituting Eq. (3.3) in Eq. (3.1) and using the fact that in this regime $N \sim (R/a)^D$ one finds for the growth of the radius of gyration[13]

$$R(c_0,t) \sim (D_f c_0 a^D t)^{1/(2+D-d)} \tag{3.4}$$

and for the cluster size

$$N(c_0,t) \sim a^{-D}(D_f c_0 a^D t)^{D/(2+D-d)}. \tag{3.5}$$

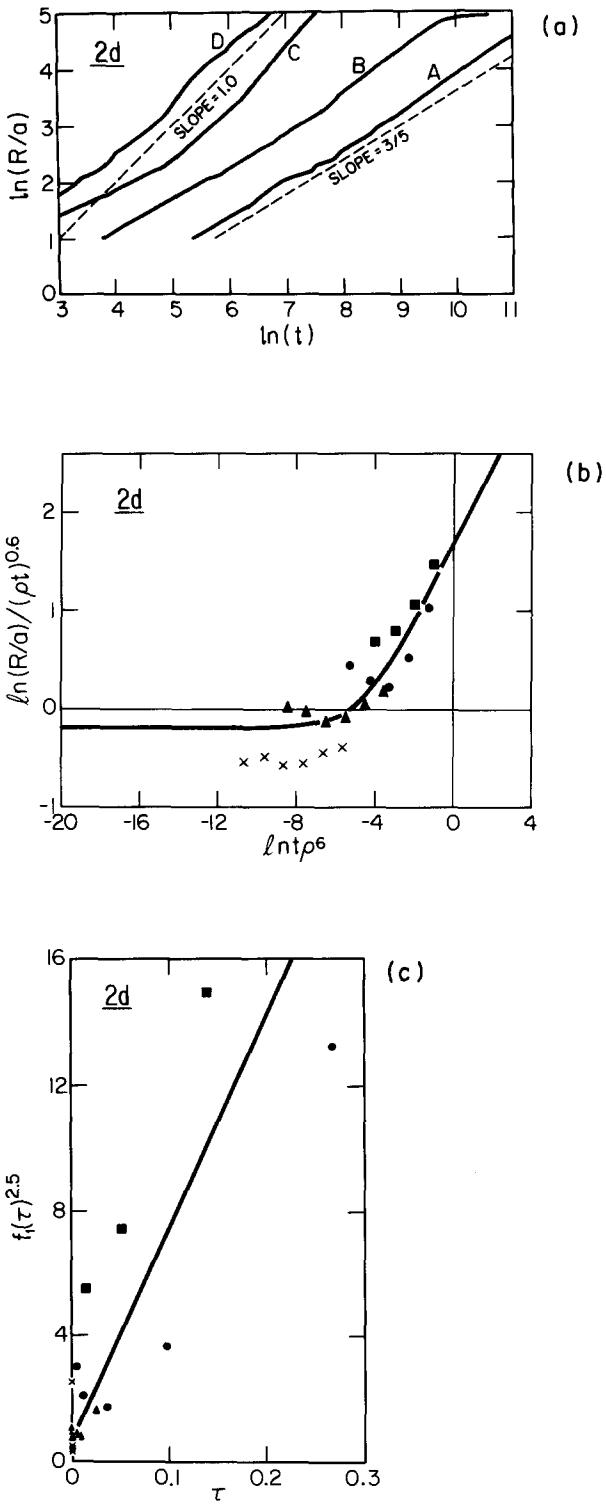

FIG. 2. (a) This figure shows how the radius of gyration, in the two dimensional case, increases with time measured in units of Monte Carlo trials per particle τ_0. The bath concentration per lattice site ρ is the same as in Fig. 1(a). The straight line with slopes 1 and 3/5 show the limiting growth laws for the cluster at long and short times. (b) Data points from the four curves A(×), B(▲), C(●), D(■) have been replotted here using the scaling variables $(R/a)/(\rho t)^{1/(2+D-d)}$ vs $\tau = t\rho^{2/(d-D)}$ in a log–log form. The data should lie on a universal curve $f_1(\tau)$, where $f_1(\tau) = [A_1 + B_1\tau]^{2/5}$. This curve has also been drawn. (c) The data points from Fig. 2(b) have been replotted here using new scaling variables. Specifically $[(R/a)/(\rho t)^{1/(2+D-d)}]^{(D+2-d)/(D+1-d)}$ has been plotted against τ. The data should lie on the straight line $A_1 + B_1\tau$. For comparison the line $(0.625 + 68.2\tau)$ has been drawn. These values have also been used in Fig. 1(b).

Equations (3.4) and (3.5) can only be valid in this asymptotic regime under the conditions $d - D < 2$ and $d > 2$. For, if $d - D > 2$ the cluster would become transparent to the diffusion, while if $d = 2$ no steady state solution of Eq. (3.2) exists. Theoretically one expects $d - D < 2$ to be obeyed for all d so this condition is not constraining. On the other hand, the case $d = 2$ presents a problem though the prediction in the limit $d \to 2$ of Eqs. (3.4) and (3.5) appears to work in practice and when compared to computer simulations. Thus we shall apply our results to the case $d = 2$ although strictly speaking the analysis is not valid for this limit. Further discussion of this point can be found in Ref. 12.

B. The R>ξ regime

Here the density of the bath and aggregate particles are both the same $\sim c_0$. Thus one does not expect a concentration gradient of the type observed in the $R \ll \xi$ regime to exist. Rather the flux of particles must be due to the short-range drop in concentration of the bath particles at the surface of the aggregate. If we assume there is only one relevant length scale ξ, then $c(r)$ must change from a value of $c(R) \sim c_0$ to $c(R - \xi) \sim 0$. If this is the case, then the total flux is

$$J_2 \sim R^{d-1} D_f c_0 / \xi \tag{3.6}$$

while $N \sim c_0 R^d$. Substituting these values of N and J_2 in $dN/dt = J_2$ leads to the result for the radius of gyration

$$R(c_0,t) \sim \frac{D_f}{a}(c_0 a^d)^{1/(d-D)} \sim D_f \xi^{-1} t. \tag{3.7}$$

Equation (3.7) gives the correct asymptotic time dependence seen in computer simulations for R and predicts the strong concentration dependence $\sim c_0^{1/(d-D)}$. For the cluster size we have

$$N(c_0,t) \sim (c_0 a^d)^{1+d/(d-D)} t^d. \tag{3.8}$$

C. Dynamic scaling hypothesis

To introduce dynamic scaling, we make use of the two dimensionless variables $x = R/\xi$ and $\tau = D_f t/\xi^2$. Then we note that we can rewrite the equations for the asymptotic time dependence of the radius of gyration $R(c_0,t)$ given by Eqs. (3.4) and (3.7) as

$$x \sim \tau^{1/(2+D-d)}, \qquad x \ll 1, \tag{3.9a}$$

$$x \sim \tau, \qquad x \gg 1. \tag{3.9b}$$

We make the dynamic scaling hypothesis that for all τ:

$$R(c_0,t) = \xi (D_f t/\xi^2)^{1/(2+D-d)} f_1(D_f t/\xi^2)$$
$$= \xi F(D_f t/\xi^2), \tag{3.10a}$$

or

$$x = \tau^{1/(2+D-d)} f_1(\tau) = F(\tau), \tag{3.10b}$$

where $f_1(\tau)$ shows the deviation from the short time behavior while $F(\tau)$ gives the complete time dependence of the growth of the radius of gyration. A form for $f_1(\tau)$ may be found in two different ways.

First, we may assume that the growth of the aggregate at all times including the crossover regime can be treated as due to the absorption of the sum of the fluxes J_1 and J_2 given by Eqs. (3.3) and (3.6), respectively;

$$\frac{dN}{dt} = J_1 + J_2 = k_1 D_f c_0 R^{d-2} + k_2 D_f c_0^{d-1}/\xi, \quad (3.11)$$

where k_1 and k_2 are dimensionless constants. In terms of the scaling variables x and τ and Eq. (2.4) for the cluster size N:

$$\frac{dG}{dx}\frac{dx}{d\tau} = k_1 x^{d-2} + k_2 x^{d-1}. \quad (3.12)$$

This equation can be integrated to yield an implicit equation for the dynamical structure function F:

$$\int_0^{F(\tau)} \frac{dG/dx}{[k_1 x^{d-2} + k_2 x^{d-1}]} dx = \tau \quad (3.13)$$

in terms of the static structure function G. If the form given by Eq. (2.5) is substituted in expression (3.13), then the integral can be numerically integrated to determine $F(\tau)$.

A second and simpler approach for determining the dynamical structure factor is simply to fit the logarithmic derivative of f_1 to a Padé approximant. Since

$$d\ln f_1/d\tau \to [1 - 1/(D+2-d)]/\tau, \quad as\ \tau \to \infty,$$

we choose the simplest Padé

$$d\ln f_1/d\tau = [1 - 1/(D+2-d)]/(\alpha + \tau)$$

which leads to

$$f_1(\tau) = (A_1 + B_1\tau)^{1-1/(D+2-d)},$$
$$F(\tau) = \tau^{1/(D+2-d)}(A_1 + B_1\tau)^{1-1/(D+2-d)}. \quad (3.14)$$

The constants A_1 and B_1 can be found from computer simulations or by comparing the asymptotic forms of Eqs. (3.13) and (3.14). In this latter case, in terms of the constants appearing in Eq. (2.5) one finds $A_1 = [(D+2-d)k_1/DA^2]^{(D+2-d)/(D+1-d)}$ and $B_1 = [k_2/dB^{d-D}]^{(D+2-d)/(D+1-d)}$.

The scaling form of the cluster size $N(c_0,t)$ with time now follows immediately from the static scaling behavior of the cluster size $N(c_0,R)$ with radius of gyration R as given in Eq. (2.4) and the dynamic scaling of the radius of gyration with time as given by Eq. (3.10):

$$N(c_0,t)/(\xi/a)^D = G[F(\tau)] = \tau^{D/(2+D-d)} f_2(\tau). \quad (3.15)$$

If we substitute in Eq. (3.15) the expressions for the structure functions G and F given by Eqs. (2.5) and (3.14), respectively, we arrive at an expression albeit complicated, for the scaling form of $N(c_0,t)/(\xi/a)^D$. A simpler satisfactory expression can be found by again simply fitting the logarithmic derivatives of $f_2(\tau)$ to a Padé approximant. As $d\ln f_2/d\tau \to$ constant as $\tau \to 0$ and $d\ln f_2/d\tau \to [d - D/(2+D-d)]/\tau$ as $\tau \to \infty$, we then have $f_2(\tau) = [A_2 + B_2\tau]^{d-D/(2+D-d)}$ or

$$N(c_0,t)/(\xi/a)^D = \tau^{D/(2+D-d)}[A_2 + B_2\tau]^{d-D/(2+D-d)}, \quad (3.16)$$

where A_2 and B_2 can be related to the constants A,B,A_1,B_1 by fitting the asymptotic forms of expression (3.16) to that for $G[F(\tau)]$ with the result

$$A_2^{d-D/(2+D-d)} = A^{d-D} A_1^{D[1-1/(2+D-d)]}, \quad (3.17)$$
$$B_2^{d-D/(2+D-d)} = B^{d-D} B_1^{d[1-1/(2+D-d)]}.$$

Next, we compare the predictions of dynamical scaling with computer simulations of these diffusion-limited fractals.

In Fig. 2(a) the radius of gyration R is plotted against t in a log–log form for two dimensions. Four clear slopes are observed for the four different concentrations A,B,C,D. In Fig. 2(b) we have replotted the data in the form $(R/a)/(\rho t)^{1/(2+D-d)}$ [with $1/(2+D-d) = 0.6$] vs $t\rho^{2/(d-D)}$ [with $2/(d-D) = 6$] in a log–log form. If dynamical scaling holds, the data should fall on a universal curve. This seems to be the case within experimental error. We have also drawn the theoretical prediction for this universal curve which is $\ln f_1(\tau)$, where $f_1(\tau) = [A_1 + B_1\tau]^{1-1/(D+2-d)}$, where $1 - 1/(D+2-d) = 0.4$. To find A_1 and B_1 we have taken the data in Fig. 2(b) to the (5/2)th power and again plotted against $t\rho^{2/(d-D)}$. In this case theory predicts that the data should fall on the universal straight line $(A_1 + B_1\tau)$. The result is presented in Fig. 2(c) together with the straight line $(0.625 + 68.2\tau)$. These values for A_1 and B_1 are also used in Fig. 2(b).

Scaling should also apply to the cluster size $N(c_0,t)$. In Fig. 3(a) can be seen an original computer simulation for the

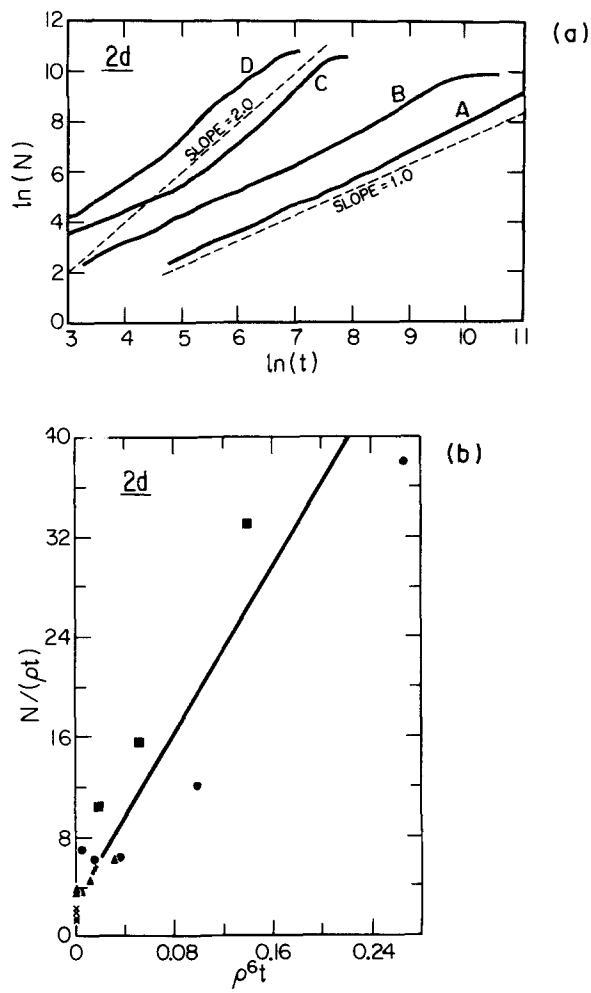

FIG. 3. (a) The time dependence of the cluster size $N(c_0,t)$. The time t is measured in units of Monte Carlo triads per particle τ_0, and the data has been plotted in a log–log form. The curves A,B,C, and D have the same meaning as in Fig. 1(a). The straight lines with slopes of 1.0 and 2.0 represent the limiting short and long time growth laws for the cluster. (b) Data from the curves A(×), B(▲), C(●), D(■) of Fig. 3(a) are replotted using the scaling variables $N/\rho t$ vs $\tau = \rho^6 t$. Theoretically these should fall on a universal straight line. This straight line $f_2(\tau) = A_2 + B_2\tau$ has been drawn with A_2 and B_2 given by Eq. (3.17).

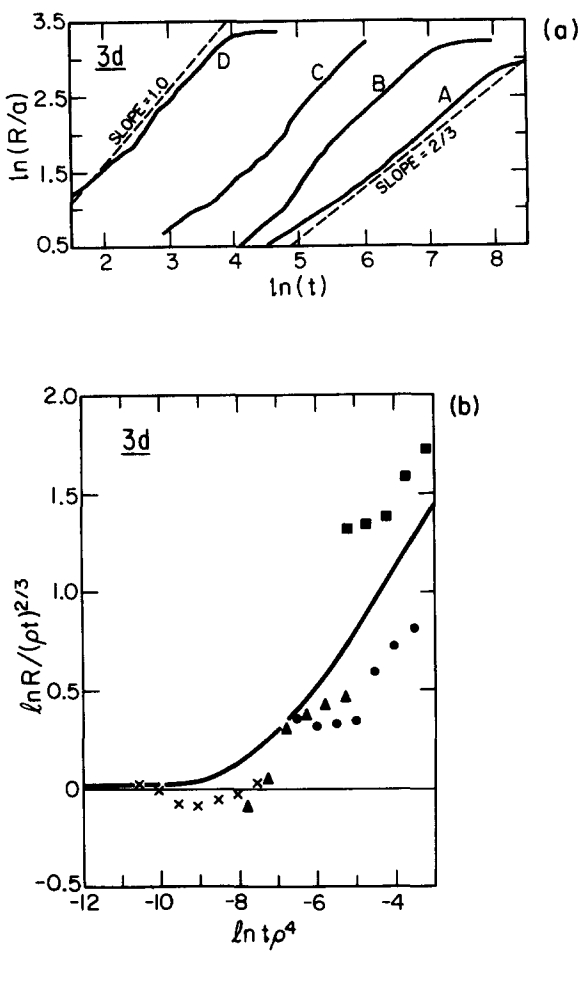

FIG. 4. (a) The growth of the radius of gyration $R(c_0,t)$ with time on a three dimensional cubic $60\times60\times60$ lattice. The data are plotted in a log–log form. The initial conditions were 5000 particles for curve A ($\rho = 0.0231$), 10 000 particles for curve B ($\rho = 0.0463$), 20 000 particles for curve C ($\rho = 0.0926$), and 40 000 particles for curve D ($\rho = 0.185$). The straight lines with slopes 2/3 and 1.0 represent the asymptotic short and long time slopes expected. (b) Data from curves A(×), B(▲), C(●), D(■) of Fig. 4(a) have been replotted here in a log–log form using the scaling variables $R/(\rho t)^{1/(2+D-d)}$ vs $\tau = t\rho^4$. The data should fall on a universal curve $\ln f_1(\tau)$, where $f_1(\tau) = [A_1 + B_1\tau]^{1/3}$. Such a curve has been drawn with $A_1 = 1.0$ and $B_1 = 1500$.

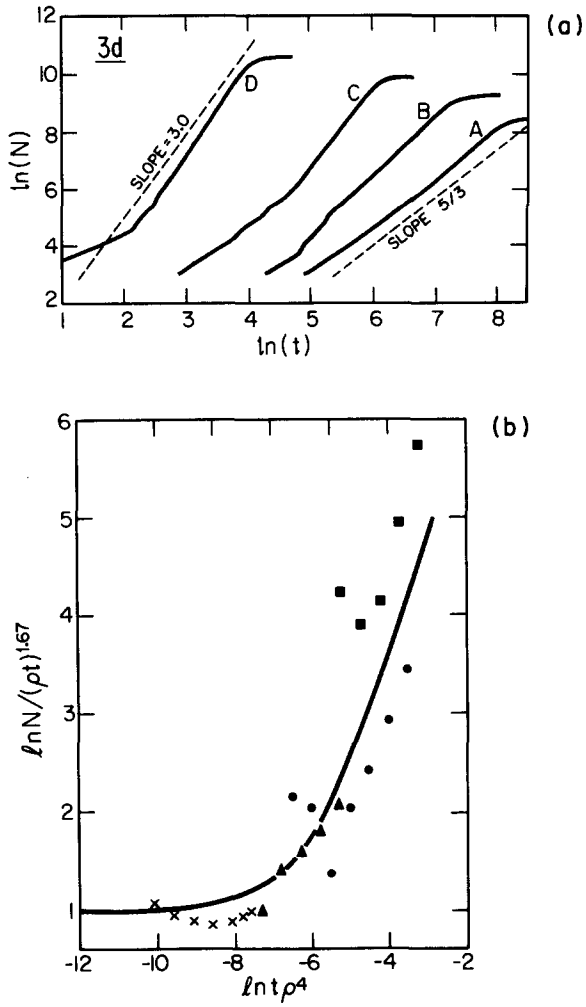

FIG. 5. (a) This figure shows the original computer simulations on a three dimensional lattice of the growth of the cluster size $N(c_0,t)$ with time. The data are plotted in a log–log form, and the curves A,B,C, and D have the same concentrations as in Fig. 4(a). The slopes of the limiting growth rates of 5/3 at short times and 3.0 at long times are also drawn. (b) Data points from curves A(×), B(▲), C(●), D(■) of Fig. 5(a) have been replotted here in a log–log form using the scaled variables $N/(\rho t)^{D/(2+D-d)}$ vs $\tau = t\rho^{2/(d-D)}$. The data should fall on a universal curve $\ln f_2(\tau)$, where $f_2(\tau) = [A_2 + B_2\tau]^{4/3}$. The curve drawn for comparison has $A_2 = 2.1$ and $B_2 = 700$.

cluster size N vs time t. Again four distinct curves can be seen while in Fig. 3(b) we have plotted $N/(\rho t)$ against $t\rho^{2/(d-D)}$. Theory makes three increasingly severe predictions about the replotted data in Fig. 3(b). First, the data should lie on a universal curve. Second, that curve should be a straight line (for the two dimensional case, if the use of the simplest Padé approximant is valid). Third, the intercept and slope of this curve A_2 and B_2, respectively, should be given by Eq. (3.17). In Fig. 3(b) we have plotted this straight line $f_2(\tau) = [A_2 + B_2\tau]$ with the values of A_2 and B_2 given by Eq. (3.17). The agreement is satisfactory.

Next, we consider three dimensions. In Fig. 4(a) the radius of gyration R is plotted in a log–log form against line t. Four curves, A,B,C,D can be seen. Here curve A has a density per lattice site $\rho = (c_0 a^3)$ of 0.0231, curve B has $\rho = 0.0463$, curve C has $\rho = 0.0926$, and curve D has $\rho = 0.185$. Points from the four curves A(×), B(▲), C(●), D(■) have been replotted in Fig. 4(b) using the scaling variables $(R/a)/(\rho t)^{1/(2+D-d)}$ with $1/(2+D-d) = 2/3$ vs $\tau = t\rho^{2/(d-D)}$ [with $2/(d-D) = 4$] in a log–log form. The data should again fall on a universal curve. In this case better agreement with the theoretical curve also drawn in Fig. 4(b) would be welcome for but scaling does appear to hold. The theoretical curve in this case is $\ln f_1(\tau)$ where $f_1(\tau) = [A_1 + B_1\tau]^{1/3}$ and $A_1 = 1.0$, $B_1 = 1500$ were used in Fig. 4(b).

In Fig. 5(a) the original computer simulation on the cluster size N vs time t is plotted in a log–log form for the three dimensional case. In Fig. 5(b) the data has been replotted using the scaled variables $N/(\rho t)^{D/(2+D-d)}$ [with $D/(2+D-d) = 5/3$] vs $\tau = t\rho^{2/(d-D)}$ [with $2/(d-D) = 4$]. Again the data should fall on a universal curve. The theoretical prediction for this curve is $\ln f_2(\tau)$ and this has also been drawn in Fig. 5(b) where we have used

$f_2(\tau) = [2.1 + 700\tau]^{4/3}$. The scaling is not good but it does appear to exist.

IV. SUMMARY

In this paper we have investigated the growth of diffusion limited clusters in a medium of particles of concentration c_0. We have employed the length scale $\xi \sim c_0^{-1/(d-D)}$ to define a static scaling function for the cluster. A simple Padé approximant for the static scaling function fits the computer simulation data rather well [see Figs. 1(b) and 1(c)]. We have also examined dynamic scaling in order to describe the kinetics of cluster growth. While agreement between the dynamic scaling predictions and the computer simulation is not exceptional (see Figs. 2–5), dynamical scaling appears to hold. Further simulations may reveal new insights into the growth of diffusion limited aggregates. For instance does dynamic scaling breakdown at large enough bath concentrations when ξ would become small?

ACKNOWLEDGMENT

This work is supported in part by the National Science Foundation under Grant No. CHE 8116613.

[1]T. A. Witten and L. M. Sander, Phys. Rev. Lett. **47**, 1400 (1981).
[2]P. Meakin, Phys. Rev. A **27**, 1495 (1983).
[3]B. B. Mandelbrot, *The Fractal Geometry of Nature* (Freeman, San Francisco, 1982).
[4]M. Muthukumar, Phys. Rev. Lett. **50**, 839 (1983).
[5]M. Tokuyama and K. Kawasaki, Phys. Lett. A **100**, 337 (1984).
[6]H. G. E. Hentschel, Phys. Rev. Lett. **52**, 212 (1984).
[7]D. M. Sutherland and I. Goodarz-Nia, Chem. Eng. Sci. **26**, 2071 (1971).
[8]P. Meakin, Phys. Rev. Lett. **51**, 1119 (1983).
[9]M. Kolb, R. Botet, and R. Jullien, Phys. Rev. Lett. **51**, 1123 (1983).
[10]H. G. E. Hentschel and J. M. Deutch, Phys. Rev. A **29**, 1609 (1984).
[11]P. Meakin and T. A. Witten, Jr. Phys. Rev. B **28**, 5632 (1983).
[12]P. Meakin and J. M. Deutch, J. Chem. Phys. **80**, 2982 (1984).
[13]J. M. Deutch and P. Meakin, J. Chem. Phys. **78**, 2093 (1983).
[14]R. Ball, M. Nauenberg, and T. Witten, Institute of Theoretical Physics (Santa Barbara) Report No NSF-ITP-83-37.
[15]M. Nauenberg, R. Richter, and L. M. Sander, Phys. Rev. B **28**, 1649 (1983).
[16]See, for instance, H. E. Stanley, *Introduction to Phase Transitions and Critical Phenomena* (Oxford University, Oxford, 1971).